

Properties of light resonances from unitarized Chiral perturbation theory: N_c behavior and quark mass dependence

J. R. PELÁEZ^{a,*}, J. NEBRED^a, G. RÍOS^a

^a*Dept. de Física Teórica II. Universidad Complutense. 28040 Madrid. Spain*

We review the unitarization of Chiral Perturbation Theory with dispersion relations and how it describes meson-meson scattering data, generating light resonances whose mass, width and nature can be related to QCD parameters like quark masses and the number of colors.

§1. Introduction

Light hadron spectroscopy lies beyond the applicability of perturbative QCD. However, there is an effective field theory, known as Chiral Perturbation Theory¹⁾ (ChPT), which provides a description of the dynamics of the lightest mesons. Despite it is limited to low energies and masses, here we review how, when combined with dispersion relations, it leads to a successful description of meson dynamics, generating resonant states without a priori assumptions on their existence or nature. This “unitarized ChPT” is a useful tool to identify the spectroscopic nature of resonances through their dependence on the QCD number of colors N_c , but also to relate lattice results to physical resonances by studying their quark mass, m_q , dependence.

ChPT is built out of the Goldstone Bosons of the QCD spontaneous chiral symmetry breaking, namely, pions, kaons and etas, as a low energy expansion of a Lagrangian respecting all QCD symmetries. It is organized in powers of p^2/Λ^2 , where p stands either for derivatives, momenta or meson masses, and $\Lambda \equiv 4\pi f_\pi$, where f_π denotes the pion decay constant. ChPT is renormalized order by order by absorbing loop divergences in the renormalization of parameters of higher order counterterms, known as low energy constants (LECs) that *carry no energy or mass dependence* and depend on a regularization scale μ . As always after renormalization, the full amplitude is independent of this scale. Their values depend on the QCD dynamics, and are determined from experiment. Up to the desired order, the ChPT expansion provides a *systematic and model independent* description of how meson observables depend on QCD parameters like the light quark masses $\hat{m} = (m_u + m_d)/2$ and m_s , or the leading $1/N_c$ behavior.²⁾

§2. Dispersion relations and unitarization

Elastic resonances appear as poles on the second Riemann sheet of the meson-meson scattering partial waves t_{IJ} of definite isospin I and angular momentum J . At physical values of s , elastic unitarity implies

$$\text{Im } t_{IJ}(s) = \sigma(s) |t_{IJ}(s)|^2 \Rightarrow t_{IJ} = \frac{1}{\text{Re } t_{IJ}^{-1} - i\sigma}, \quad \text{with } \sigma(s) = 2p/\sqrt{s}, \quad (2.1)$$

^{*)} speaker. J.R.P. thanks the NFQCD2010 organizers for the invitation and for their work to create such an exciting workshop.

where s is the Mandelstam variable and p is the center of mass momentum. However, ChPT amplitudes, being an expansion $t_{IJ} \simeq t_{IJ}^{(2)} + t_{IJ}^{(4)} + \dots$, with $t^{(2k)} = O(p^{2k})$, can only satisfy Eq. (2.1) perturbatively

$$\text{Im } t_{IJ}^{(2)}(s) = 0, \text{Im } t_{IJ}^{(4)}(s) = \sigma(s)|t_{IJ}(s)^{(2)}|^2, \dots \Rightarrow \text{Im } t_{IJ}^{(4)}(s)/t_{IJ}^{(2)2}(s) = \sigma(s), \quad (2.2)$$

and cannot generate poles. However, the resonance region can be reached combining ChPT with dispersion theory either for the amplitude³⁾ or for the inverse amplitude through the Inverse Amplitude Method (IAM).⁴⁾⁻⁶⁾ We will concentrate on the *one-channel* IAM,^{4),5)} since it uses ChPT only up to a given order inside a dispersion relation, without additional input or further model dependent assumptions. Other unitarization techniques will be commented below.

2.1. The one-loop ChPT Inverse Amplitude Method

For a partial wave $t_{IJ}(s)$, we can write a dispersion relation (that we subtract three times, since we will also use it below for $t_{IJ}^{(4)}$, that grows with s^2)

$$t_{IJ}(s) = C_0 + C_1 s + C_2 s^2 + \frac{s^3}{\pi} \int_{s_{th}}^{\infty} \frac{\text{Im } t_{IJ}(s') ds'}{s'^3(s' - s - i\epsilon)} + LC(t_{IJ}). \quad (2.3)$$

Note we have explicitly written the integral over the physical cut, extending from threshold, s_{th} , to infinity, but we have abbreviated by LC the equivalent expression for the left cut (from 0 to $-\infty$). We could do similarly with other cuts, if present, as for $\pi K \rightarrow \pi K$. Note that from Eq.(2.1) the imaginary part of the *inverse amplitude* is *exactly* known in the elastic regime. We can then write a dispersion relation like that in (2.3) but now for the auxiliary function $G = (t_{IJ}^{(2)})^2/t_{IJ}$, i.e.,

$$G(s) = G_0 + G_1 s + G_2 s^2 + \frac{s^3}{\pi} \int_{s_{th}}^{\infty} \frac{\text{Im } G(s') ds'}{s'^3(s' - s - i\epsilon)} + LC(G) + PC,$$

where now PC stands for possible pole contributions in G coming from zeros in t_{IJ} . It is now straightforward to expand the subtraction constants and use that $\text{Im } t_{IJ}^{(2)} = 0$ and $\text{Im } t_{IJ}^{(4)} = \sigma|t_{IJ}^{(2)}|^2$, so that $\text{Im } G = -\text{Im } t_{IJ}^{(4)}$. In addition, up to the given order, $LC(G) \simeq -LC(t_{IJ}^{(4)})$, whereas PC is of higher order and can be neglected. Then

$$\frac{t_{IJ}^{(2)2}}{t_{IJ}} \simeq a_0 + a_1 s - b_0 - b_1 s - b_2 s^2 - \frac{s^3}{\pi} \int_{s_{th}}^{\infty} \frac{\text{Im } t_{IJ}^{(4)}(s') ds'}{s'^3(s' - s - i\epsilon)} - LC(t_{IJ}^{(4)}) \simeq t_{IJ}^{(2)} - t_{IJ}^{(4)},$$

since the a_i, b_i terms, coming from the G_i expansion, are the subtraction terms of a dispersion relation for $t_{IJ}^{(2)} - t_{IJ}^{(4)}$. Thus we arrive at the so-called IAM:

$$t_{IJ} \simeq t_{IJ}^{(2)2}/(t_{IJ}^{(2)} - t_{IJ}^{(4)}), \quad (2.4)$$

that provides an elastic amplitude satisfying unitarity and has the correct ChPT expansion up to the order we have used. The PC contribution has been calculated explicitly⁶⁾ and is not just formally suppressed, but numerically negligible except near the Adler zeros, away from the physical region. It is straightforward to extend

the IAM to other elastic channels or higher orders.⁵⁾ Naively, the IAM looks like replacing $\text{Re } t_{IJ}^{-1}$ by its $O(p^4)$ ChPT expansion in (2.1), but (2.1) is only valid in the real axis, whereas our derivation allows us to consider the amplitude in the complex plane and look for poles associated to resonances. Let us remark that, since ChPT is used *only at low energies* in the dispersion relation, the IAM formula is justified only up to energies where inelasticities become important, even though ChPT does not converge at those energies. Only when the energy is close to the Adler zero one should use a slightly modified version of the IAM.⁶⁾ Re-expanding the IAM, ChPT is recovered up to the order it was used as input, as well as partial contributions to higher order, but not the complete series— see Ref.7) for a discussion of this issue.

In Fig.1 we present some results⁸⁾ of an updated fit of the IAM $\pi\pi$ and πK scattering amplitudes to data, simultaneously fitting the available lattice results on ratios of meson masses and decay constants and some scattering lengths. It is important to remark that the resulting LECs are in fairly good agreement with standard determinations: no fine tuning is required. The $f_0(600)$, $\rho(770)$, $\kappa(800)$ and $K^*(892)$ are *not introduced by hand* but *generated* as poles in the second Riemann sheet of their corresponding partial waves. The fact that we do not need to model the integrands and *the only input parameters are those of ChPT* is relevant since we then know how to relate our amplitudes to QCD parameters like N_c or m_q .

2.2. Other unitarization techniques within the coupled channel formalism

Naively one can arrive at (2.4) in a matrix form, ensuring coupled channel unitarity, just by expanding the real part of the inverse T matrix. Unfortunately, *there is still no dispersive derivation* including a left cut *for the coupled channel case*. Being much more complicated, different approximations to $\text{Re } T^{-1}$ have been used:

- The fully renormalized one-loop ChPT calculation of $\text{Re } T^{-1}$ provides the correct ChPT expansion, with left cuts approximated to $O(p^4)$.^{10),12)} Indeed, using LECs consistent with standard ChPT determinations, one can describe¹⁰⁾ below 1.2 GeV all two-body scattering channels made of pions, kaons or etas. Simultaneously, this approach¹⁰⁾ generates poles associated to the $\rho(770)$ and $K^*(892)$ vector mesons, together with the $f_0(980)$, $a_0(980)$, $f_0(600)$ and κ (or $K_0(800)$) scalar resonances.

- Originally,¹³⁾ the coupled channel IAM was used neglecting crossed loops and tadpoles. This is considerably simpler, and despite the left cut is absent, since its numerical influence is relatively small, meson-meson data are described with reasonable LECs while generating all poles enumerated above. Note that this approximation keeps the s-channel loops but also the tree level up to $O(p^4)$, which encodes the effect of heavier resonances, like the ρ . Thus, contrary to some common belief, the IAM incorporates the low energy effects of t-channel ρ exchange.

- Finally, if only scalar meson-meson scattering is of interest, it is possible to use just one cutoff (or another regulator) that numerically mimics the combination of LECs appearing in scalar channels. This "chiral unitary approach" is very popular, even beyond the meson-meson framework, due to its great simplicity but remarkable success¹⁴⁾ and also for its straightforward relation to the Bethe-Salpeter formalism¹⁵⁾ that provides physical insight on unitarization. With this method it was shown¹⁶⁾ that, assuming no m_q dependence of the cutoff, all light scalar resonances degenerate

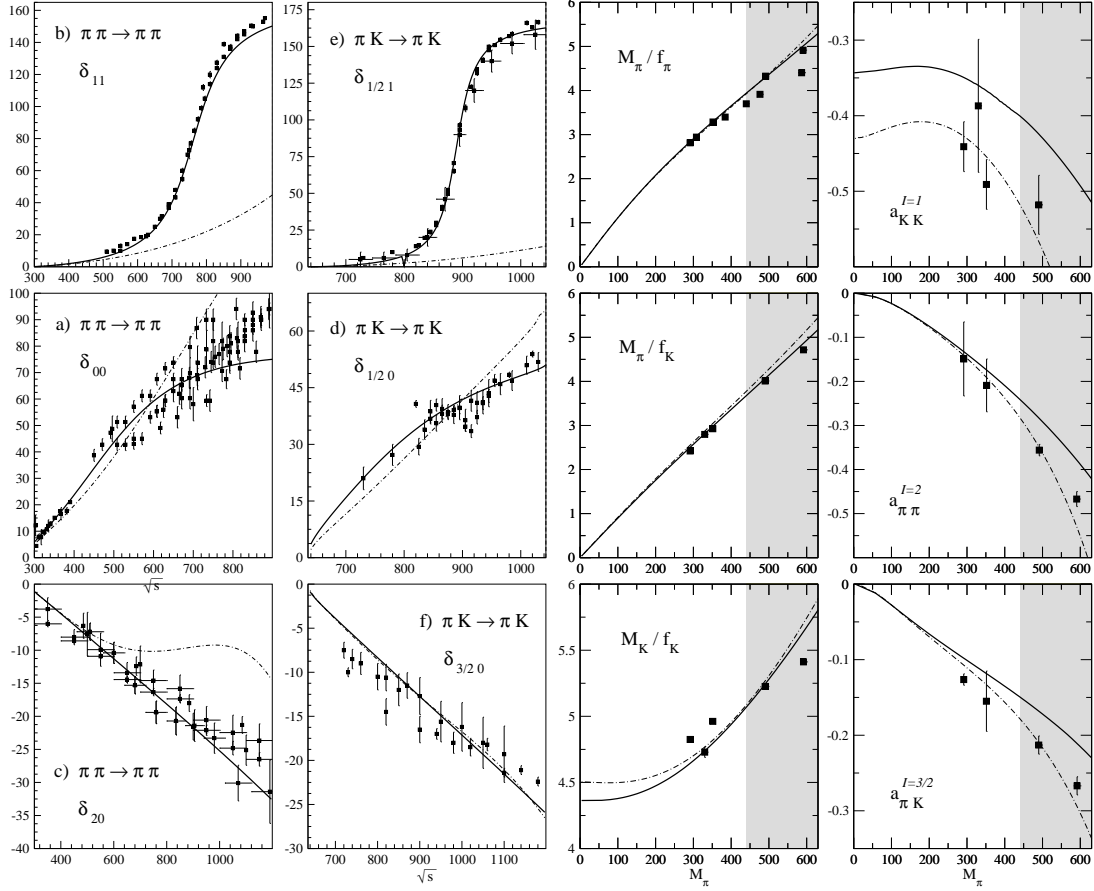


Fig. 1. Updated IAM fit⁸⁾ (continuous line). We also show non-unitarized ChPT results with the LECs from the K_{l4} two-loop analysis⁹⁾ (dot-dashed line). **Left:** IAM versus data on $\pi\pi$ and πK scattering. **Right:** fit results compared to lattice calculations¹¹⁾ on ratios of meson masses and decay constants and some scattering lengths. We fit up to $m_\pi = 440$ MeV, but even beyond (grey areas) lattice results are not described badly. Experimental references are detailed in 10).

into an octet and a singlet in the $SU(3)$ limit. Axial-vector mesons have also been generated by using a chiral Lagrangian for the pseudoscalar-vector interaction.¹⁷⁾

§3. The nature of resonances from their leading $1/N_c$ behavior

The QCD $1/N_c$ expansion,²⁾ valid in the whole energy region, provides a rigorous definition of $\bar{q}q$ bound states: their masses and widths behave as $O(1)$ and $O(1/N_c)$, respectively. The QCD leading $1/N_c$ behavior of f_π and the LECs is well known, and ChPT amplitudes have no cutoffs or subtraction constants where spurious N_c dependences could hide. Hence, by scaling with N_c the ChPT parameters in the IAM, the N_c dependence of the mass and width of the resonances has been determined to one and two loops.^{18),19)} These are defined from the pole position as $\sqrt{s_{pole}} = M - i\Gamma$. However, *a priori*, one should be careful not to take N_c too large, because the $N_c \rightarrow \infty$ limit is a weakly interacting limit. As shown above, the IAM relies on the fact that the exact elastic RC contribution dominates the dispersion relation. Since the

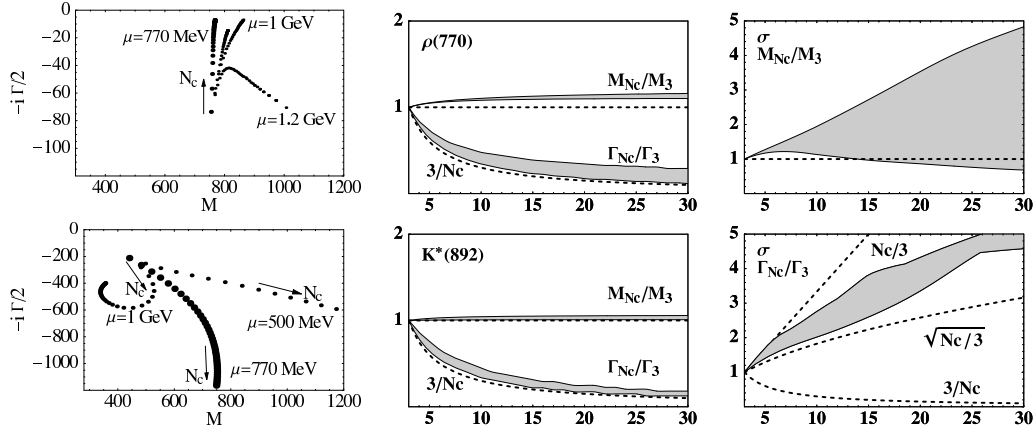


Fig. 2. **Left:** ρ (top) and σ (bottom) pole trajectories for different values of μ , note that for $\mu = 1.2$ GeV the ρ pole goes away the real axis. **Center:** N_c behavior of the ρ (top) and K^* (bottom) mass and width. **Right:** N_c behavior of the σ mass and width.

IAM describes data and the resonances within, say, 10 to 20% errors, this means that at $N_c = 3$ the other contributions are not approximated badly. But meson loops, responsible for the RC , scale as $3/N_c$ whereas the inaccuracies due to the approximations scale partly as $O(1)$. Thus, we can estimate that those 10 to 20% errors at $N_c = 3$ become 100% errors at, say $N_c \sim 30$ or $N_c \sim 15$, respectively. Hence we never show results^{18),19)} beyond $N_c = 30$. Even beyond $N_c \sim 15$ they should be interpreted with care.

Thus, Fig.2 shows the behavior of the ρ , K^* and σ masses and widths found in.¹⁸⁾ The ρ and K^* neatly follow the expected behavior for a $\bar{q}q$ state: $M \sim 1$, $\Gamma \sim 1/N_c$. The bands cover the uncertainty $\mu \sim 0.5 - 1$ GeV where to apply the $1/N_c$ scaling. Note also that *outside this μ range* the ρ meson starts deviating from a $\bar{q}q$ behavior. Something similar occurs to the $K^*(892)$. Hence, we cannot apply the N_c scaling at an arbitrary μ value, if the well established ρ and K^* $\bar{q}q$ nature is to be reproduced.

In contrast, the σ shows a different behavior from that of a pure $\bar{q}q$: *near $N_c=3$* both its mass and width grow with N_c , i.e. its pole moves away from the real axis. Of course, far from $N_c = 3$, and for some choices of LECs and μ , the σ pole might turn back to the real axis,^{19)–21)} as seen in Fig.2 (top-right). But, as commented above, the IAM is less reliable for large N_c , and at most this behavior only suggests that there *might be* a subdominant $\bar{q}q$ component.¹⁹⁾ In addition, we have to ensure that the LECs fit data and reproduce the vector $\bar{q}q$ behavior.

Since loops are important in determining the scalar pole position, but are $1/N_c$ suppressed compared to tree level terms with LECs, we checked the $O(p^4)$ results with an $O(p^6)$ IAM calculation in $SU(2)$.¹⁹⁾ We defined a χ^2 -like function to measure how close a resonance is from a $\bar{q}q$ N_c behavior. First, we used it at $O(p^4)$ to show that it is not possible for the σ to behave predominantly as a $\bar{q}q$ while describing simultaneously the data and the ρ $\bar{q}q$ behavior, thus *confirming the robustness of the conclusions for N_c close to 3*. Next, we obtained a $O(p^6)$ data fit where the ρ $\bar{q}q$ behavior was imposed (see Fig.3, left and center). Note that both M_σ and Γ_σ grow with N_c near $N_c = 3$, confirming the $O(p^4)$ result of a non $\bar{q}q$ dominant

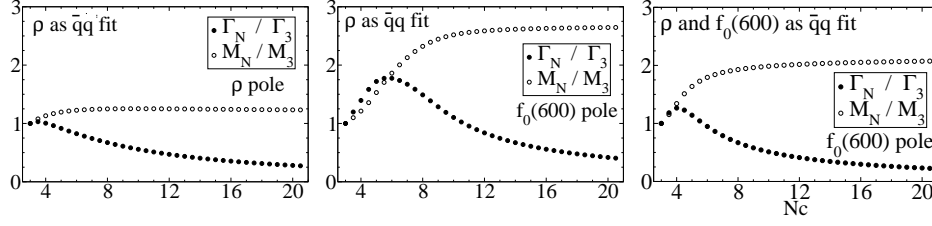


Fig. 3. **Left and center:** N_c behavior of the ρ and σ pole at $O(p^6)$ with the “ ρ as $\bar{q}q$ fit”. **Right:** Sigma behavior with N_c at $O(p^6)$ with the “ ρ and σ as $\bar{q}q$ fit”.

component. However, for N_c between 8 and 15, where we still trust the IAM, M_σ becomes constant and Γ_σ starts decreasing. This may hint to a *subdominant $\bar{q}q$ component*, arising as loops become suppressed when N_c grows. Finally, by forcing the σ to behave as a $\bar{q}q$, we found that in the best case (Fig.3, right) this subdominant $\bar{q}q$ component could become dominant around $N_c > 6 - 8$, at best, but always with an $N_c \rightarrow \infty$ mass above ~ 1 GeV instead of its physical ~ 450 MeV value.

Let us emphasize again²²⁾ what can and *what cannot* be concluded from our results and clarify some frequent questions and doubts:

- Most likely, scalars are a mixture of different states, but *the dominant component of the σ and κ in meson-meson scattering does not behave as a $\bar{q}q$* . If the $\bar{q}q$ was dominant, they would behave as the ρ or the K^* in Fig.2. However, a smaller fraction of $\bar{q}q$ cannot be excluded and is somewhat favored in our $O(p^6)$ analysis.¹⁹⁾
- Two meson and some tetraquark states²³⁾ have a consistent “qualitative” behavior, i.e., both disappear in the meson-meson scattering continuum as N_c increases. Our results are not able yet to establish the nature of that dominant component. To do so other tools^{28), 29)} might be necessary. The most we can state is that the behavior of two-meson states or some tetraquarks might be qualitatively consistent.

The $N_c \rightarrow \infty$ limit has been studied in 20), 21). Apart from its mathematical interest, it could have some physical relevance if the data and the large N_c uncertainty on the choice of scale were more accurate. Nevertheless:

- *A priori the IAM is not reliable in the $N_c \rightarrow \infty$ limit*, since that is a weakly interacting theory, where exact unitarity becomes less relevant in confront of other approximations made in the IAM derivation. It has been shown²⁰⁾ that it might work well in that limit in the vector channel of QCD but not in the scalar channel.
- Another reason to keep N_c not too far from 3 is that we have not included the $\eta'(980)$, whose mass is related to the $U_A(1)$ anomaly and scales as $\sqrt{3/N_c}$. Nevertheless, if in our calculations we keep $N_c < 30$, its mass would be > 310 MeV and thus pions are still the only relevant degrees of freedom in the σ region.
- *Contrary to the leading $1/N_c$ behavior in the vicinity of $N_c = 3$, the $N_c \rightarrow \infty$ limit does not give information on the “dominant component” of light scalars*. The reason was commented above: in contrast to $\bar{q}q$ states, that become bound, two-meson and some tetraquark states dissolve in the continuum as $N_c \rightarrow \infty$. Thus, even if we started with an infinitesimal $\bar{q}q$ component in a resonance, for a sufficiently large N_c it may become dominant, and beyond that N_c the associated pole would behave as a $\bar{q}q$ state. Also, since the mixings of different components could change with N_c , a too large N_c could alter significantly the original mixings.

Actually, this is what happens for the one-loop IAM σ resonance for $N_c \rightarrow \infty$, but it does *not* necessarily mean that the “correct interpretation [...] is that the σ pole is a conventional $\bar{q}q$ meson envired by heavy pion clouds”.²¹⁾ That the σ is not conventional is simply seen by comparing it with the “conventional” ρ and K^* in Fig. 2. A large two-meson component is consistent, but so is a tetraquark. Actually, the $N_c \rightarrow \infty$ of the one-loop unitarized ChPT pole in the scalar channel limit is not unique^{20),21)} given the uncertainty in the chiral parameters. Moreover, despite the one-loop IAM could make sense in the $N_c \rightarrow \infty$ limit for the vector channel,²⁰⁾ in the scalar channel it can lead to phenomenological inconsistencies²⁰⁾ for some LECs, since poles can even move to negative squared mass values (weird), to infinity or to a positive mass square. Hence, robust conclusions on the dominant light scalar component can be obtained not too far from real life, say $N_c < 15$ or 30, for a μ choice between roughly 0.5 and 1 GeV, that simultaneously ensures the $\bar{q}q$ dependence for the ρ and K^* mesons. Note, however, that under these same conditions the two-loop IAM still finds, not only a dominant non- $\bar{q}q$ component, but also a hint of a $\bar{q}q$ subdominant component,¹⁹⁾ which is not conventional in the sense that it appears at a much higher mass than the physical σ . This subdominant component at that higher mass seems to be needed to ensure fulfillment of local duality²⁴⁾ for $N_c > 3$. This may support the existence of a second scalar octet, a $\bar{q}q$ now, above 1 GeV.²⁵⁾

Finally, using not the IAM, but the chiral unitary approach with a natural range for the cutoff N_c dependence, it has also been suggested²⁶⁾ that a large, in some cases dominant, non $\bar{q}q$ behavior could exist in axial vector mesons.

§4. Quark mass dependence of resonances

ChPT provides a rigorous expansion of meson masses in terms of m_q (at leading order $M_{meson}^2 \sim m_q$). Thus, by changing the meson masses in the amplitudes, we see how the poles generated with the IAM depend on m_q . We report here the SU(2) analysis²⁷⁾ of ρ and σ as well the SU(3) analysis⁸⁾ of non-strange, ρ and σ , and strange, $\kappa(800)$ and $K^*(892)$, resonances.

The values of m_π considered should fall within the ChPT range of applicability and allow for some elastic $\pi\pi$ and πK regime below $K\bar{K}$ or $K\eta$ thresholds, respectively. Both criteria are satisfied if $m_\pi \leq 440$ MeV, since $SU(3)$ ChPT still works with such kaon masses, and because for $m_\pi \simeq 440$ MeV, the kaon mass becomes $\simeq 600$ MeV. Of course, we expect higher order corrections, which are not considered here, to become more relevant as m_π is increased. Thus, our results become less reliable as m_π increases due to the $O(p^6)$ corrections which we have neglected.

Fig. 4 (left) shows the evolution of the σ and ρ pole positions as m_π is increased. In order to see the pole movements relative to the two pion threshold, which is also increasing, we use units of m_π , so the threshold is fixed at $\sqrt{s} = 2$. Both poles move closer to threshold and they approach the real axis. The ρ poles reach the real axis at the same time that they cross threshold. One of them jumps into the first sheet and stays below threshold in the real axis as a bound state, while its conjugate partner remains on the second sheet practically at the very same position as that in the first. In contrast, the σ poles go below threshold with a finite imaginary part

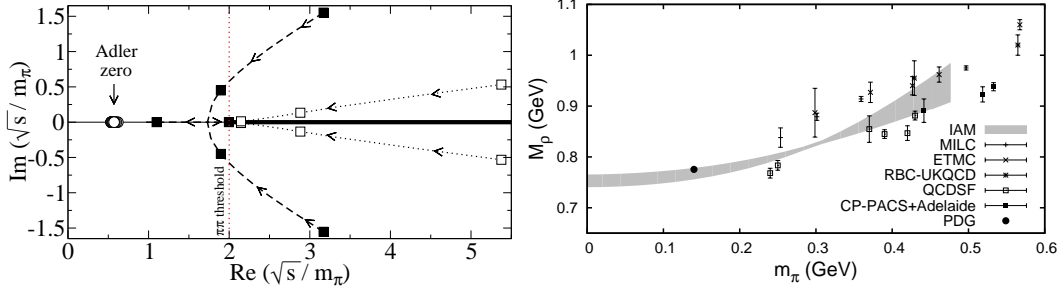


Fig. 4. **Left:** Movement of the σ (dashed lines) and ρ (dotted lines) poles for increasing m_π (direction indicated by the arrows) on the second sheet. The filled (open) boxes denote the pole positions for the σ (ρ) at pion masses $m_\pi = 1, 2$, and $3 \times m_\pi^{\text{phys}}$, respectively. For $m_\pi = 3m_\pi^{\text{phys}}$ three poles accumulate very near the threshold. All poles are always far enough from the Adler zero (circles). **Right:** Comparison of our results for the M_ρ dependence on m_π with some recent lattice results.³²⁾ The grey band covers the error coming from the LECs uncertainties.

before they meet in the real axis, still on the second sheet, becoming virtual states. As m_π increases, one pole moves toward threshold and jumps through the branch point to the first sheet staying in the real axis below threshold, very close to it as m_π keeps growing. The other σ pole moves down in energies away from threshold and remains on the second sheet. These very asymmetric poles could signal a prominent molecular component,^{28),29)} at least for large pion masses. Similar movements were found within quark models³⁰⁾ and a finite density analysis.³¹⁾

Fig. 4 (right) shows our results for the ρ mass dependence on m_π compared with some recent lattice results,³²⁾ and the PDG value for the ρ mass. Now the mass is defined as the point where the phase shift crosses $\pi/2$, except for those m_π values where the ρ becomes a bound state, where it is defined again from the pole position. Taking into account the incompatibilities between different lattice collaborations, we find a qualitative good agreement with lattice results. Note also that the m_π dependence in our approach is correct only up to NLO in ChPT, and we expect higher order corrections to be important for large pion masses. The M_ρ dependence on m_π agrees also with estimations for the two first coefficients of its chiral expansion.³³⁾

In Fig. 5 (left) we compare the m_π dependence of M_ρ and M_σ (defined from the pole position $\sqrt{s_{\text{pole}}} = M - i\Gamma/2$), normalized to their physical values. The bands cover the LECs uncertainties. Both masses grow with m_π , but M_σ grows faster than M_ρ . Below $m_\pi \simeq 2.4 m_\pi^{\text{phys}}$ we only show one line because the two conjugate σ poles have the same mass. Above $2.4 m_\pi^{\text{phys}}$, these two poles lie on the real axis with two different masses. The heavier pole goes towards threshold and around $m_\pi \simeq 3.3 m_\pi^{\text{phys}}$ moves into the first sheet, but that is beyond our applicability limit.

In the next panel of Fig. 5 we compare the m_π dependence of Γ_ρ and Γ_σ normalized to their physical values: note that both widths become smaller. We compare this decrease with the expected phase space reduction as resonances approach the $\pi\pi$ threshold. We find that Γ_ρ follows very well this expected behavior, which implies that the $\rho\pi\pi$ coupling is almost m_π independent. In contrast, Γ_σ deviates from the phase space reduction expectation. This suggests a strong m_π dependence of the σ coupling to two pions, necessarily present for molecular states.^{29),34)}

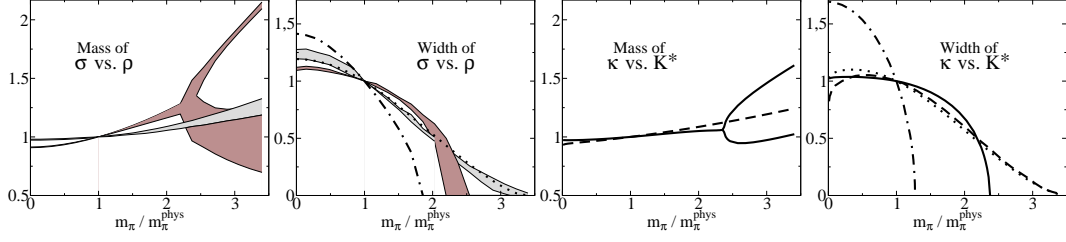


Fig. 5. m_π dependence of resonance masses and widths in units of the physical values. In the two left panels the dark (light) band shows the results for the σ (ρ). The band width reflects the uncertainties in the SU(2) LECs. Similarly, the two right panels, calculated within SU(3),⁸⁾ show the behavior for the $K^*(892)$ (continuous) and $\kappa(800)$ (dashed). The (dotted) dot-dashed line shows the m_π dependence of the corresponding vector (scalar) width from the change of phase space only, assuming a constant coupling of the resonance to two mesons.

Finally, in the last two panels of Fig.5 we compare the mass and width dependence on \hat{m} of the $\kappa(800)$ versus the $K^*(892)$, keeping m_s fixed.⁸⁾ Note that the same pattern of the $\sigma - \rho$ system is repeated. Belonging to the same octet, $K^*(892)$ and ρ behave very similarly, and both their widths follow just phase space reduction. The σ and κ behaviors are only qualitatively similar, the latter being somewhat softer. This might be partly due to a possible significant admixture of singlet state in the σ . The dependence of these resonances on m_s has been also studied in Ref.8).

§5. Summary

We have reviewed how the Inverse Amplitude Method (IAM)⁶⁾ is derived from the first principles of analyticity, unitarity, and Chiral Perturbation Theory (ChPT) at low energies. It is able to generate, as poles in the amplitudes, the light resonances appearing in meson-meson elastic scattering, without any a priori assumptions. Up to a given order in ChPT, it yields the correct dependences on \hat{m} , m_s and N_c .

The leading $1/N_c$ behavior suggests that the dominant component of light scalars does not behave as a $\bar{q}q$ state as N_c increases not far from $N_c = 3$. When using the two loop IAM result in SU(2), below $N_c \sim 15$ or 30, there is a hint of a subdominant $\bar{q}q$ component, but arising at roughly twice the mass of the physical σ .

We have studied the pion (quark) mass dependence of the $f_0(600)$, $\rho(770)$, $\kappa(800)$ and $K^*(892)$ poles^{8),27)} and how they become bound states: softly for vectors and with a non-analyticity for scalars. We found that the vector-meson-meson coupling constant is almost m_π independent and a qualitative agreement with some lattice results for the ρ mass evolution with m_π . These results may be relevant for studies of the meson spectrum³⁶⁾ and form factors³⁵⁾ on the lattice.

Acknowledgments

Work partially supported by Spanish MICINN: FPA2007-29115-E, FPA2008-00592 and FIS2006-03438, U.Complutense/ Banco Santander grant PR34/07-15875-BSCH and UCM-BSCH GR58/08 910309 and the EU-Research Infrastructure Integrating Activity “Study of Strongly Interacting Matter” (HadronPhysics2, Grant n 227431) under the EU Seventh Framework Programme.

References

- 1) S. Weinberg, *Physica* **A96** (1979) 327. J. Gasser and H. Leutwyler, *Annals Phys.* **158** (1984) 142; *Nucl. Phys. B* **250** (1985) 465.
- 2) G. 't Hooft, *Nucl. Phys. B* **72** (1974) 461. E. Witten, *Ann. Phys.* **128** (1980) 363.
- 3) I. Caprini *et al.*, *Phys. Rev. Lett.* **96** (2006) 132001. S. Descotes-Genon and B. Moussallam, *Eur. Phys. J. C* **48**, 553 (2006)
- 4) T. N. Truong, *Phys. Rev. Lett.* **61**, 2526 (1988). T. N. Truong, *Phys. Rev. Lett.* **67**, 2260 (1991). A. Dobado, M. J. Herrero and T. N. Truong, *Phys. Lett. B* **235**, 134 (1990).
- 5) A. Dobado and J. R. Peláez, *Phys. Rev. D* **47** (1993) 4883; *Phys. Rev. D* **56** (1997) 3057.
- 6) A. Gomez Nicola, J. R. Peláez and G. Rios, *Phys. Rev. D* **77**, 056006 (2008)
- 7) J. Gasser and U.-G. Meißner, *Nucl. Phys. B* **357** (1991) 90.
- 8) J. Nebreda and J. R. Peláez, *Phys. Rev. D* **81**, 054035 (2010).
- 9) G. Amoros, J. Bijnens and P. Talavera, *Nucl. Phys. B* **602**, 87 (2001)
- 10) A. Gomez Nicola and J. R. Peláez, *Phys. Rev. D* **65**, 054009 (2002). AIP Conf. Proc. **660** (2003) 102. [hep-ph/0301049]. J. R. Peláez, *Mod. Phys. Lett. A* **19**, 2879 (2004)
- 11) S. R. Beane *et al.* [NPLQCD Collaboration], *Phys. Rev. D* **77**, 094507 (2008) and *Phys. Rev. D* **77**, 014505 (2008); S. R. Beane *et al.* *Phys. Rev. D* **74**, 114503 (2006); Ph. Boucaud *et al.* [ETM collaboration], *Commun. Phys.* **179**, 695 (2008).
- 12) F. Guerrero and J. A. Oller, *Nucl. Phys. B* **537**, 459 (1999) [Erratum-ibid. *B* **602**, 641 (2001)]
- 13) J. A. Oller, E. Oset and J. R. Peláez, *Phys. Rev. Lett.* **80** (1998) 3452; *Phys. Rev. D* **59** (1999) 074001
- 14) J. A. Oller and E. Oset, *Nucl. Phys. A* **620**, 438 (1997) [Erratum-ibid. *A* **652**, 407 (1999)] and *Phys. Rev. D* **62** (2000) 114017.
- 15) J. Nieves and E. Ruiz Arriola, *Phys. Lett. B* **455**, 30 (1999)
- 16) J. A. Oller, *Nucl. Phys. A* **727**, 353 (2003)
- 17) M. F. M. Lutz and E. E. Kolomeitsev, *Nucl. Phys. A* **730**, 392 (2004). L. Roca, E. Oset and J. Singh, *Phys. Rev. D* **72**, 014002 (2005). L. S. Geng, E. Oset, L. Roca and J. A. Oller, *Phys. Rev. D* **75**, 014017 (2007).
- 18) J. R. Peláez, *Phys. Rev. Lett.* **92**, 102001 (2004).
- 19) J. R. Peláez and G. Rios, *Phys. Rev. Lett.* **97**, 242002 (2006)
- 20) J. Nieves and E. R. Arriola, *Phys. Rev. D* **80**, 045023 (2009)
- 21) Z. X. Sun, *et al.* [arXiv:hep-ph/0411375] and Z. X. Sun, *et al.* [arXiv:hep-ph/0503195].
- 22) J. R. Peláez, arXiv:hep-ph/0509284. Proceedings of the 11th International Conference on Elastic and Diffractive Scattering, Blois, France, 15-20 May 2005. J. R. Peláez and G. Rios, arXiv:0905.4689 [hep-ph]. Proceedings of Excited QCD, Zakopane, Poland, 8-14 Feb 2009.
- 23) R. L. Jaffe, Proc. of the Intl. Symposium on Lepton and Photon Interactions at High Energies. Physikalisches Institut, Univ. of Bonn (1981). ISBN: 3-9800625-0-3.
- 24) J. R. de Elvira, J. R. Peláez, M. R. Pennington and D. J. Wilson, arXiv:1001.2746 [hep-ph].
- 25) E. Van Beveren, *et al.* *Z. Phys. C* **30**, 615 (1986) and hep-ph/0606022. E. van Beveren and G. Rupp, *Eur. Phys. J. C* **22** (2001) 493, J. A. Oller and E. Oset, *Phys. Rev. D* **60** (1999) 074023. F. E. Close and N. A. Tornqvist, *J. Phys. G* **28**, R249 (2002).
- 26) L. S. Geng, E. Oset, J. R. Peláez and L. Roca, *Eur. Phys. J. A* **39**, 81 (2009)
- 27) C. Hanhart, J. R. Peláez and G. Rios, *Phys. Rev. Lett.* **100**, 152001 (2008)
- 28) D. Morgan, *Nucl. Phys. A* **543** (1992) 632; D. Morgan and M. R. Pennington, *Phys. Rev. D* **48** (1993) 1185.
- 29) V. Baru *et al.*, *Phys. Lett. B* **586** (2004) 53.
- 30) E. van Beveren *et al.*, AIP Conf. Proc. **660**, 353 (2003); *Phys. Rev. D* **74**, 037501 (2006).
- 31) D. Fernandez-Fraile, A. Gomez Nicola and E. T. Herruzo, *Phys. Rev. D* **76**, 085020 (2007)
- 32) Ph. Boucaud *et al.* [ETM Collaboration], *Phys. Lett. B* **650**, 304 (2007) C. Allton *et al.* [RBC and UKQCD Collaborations], *Phys. Rev. D* **76**, 014504 (2007) C. W. Bernard *et al.*, *Phys. Rev. D* **64**, 054506 (2001) C. R. Allton *et al.* *Phys. Lett. B* **628**, 125 (2005) M. Gockeler *et al.* [QCDSF Collaboration], [arXiv:hep-lat/0810.5337].
- 33) P. C. Bruns and U.-G. Meißner, *Eur. Phys. J. C* **40** (2005) 97.
- 34) S. Weinberg, *Phys. Rev.* **130**, 776 (1963); Y. Kalashnikova *et al.*, *Eur. Phys. J. A* **24** (2005) 437.
- 35) F. K. Guo, C. Hanhart, F. J. Llanes-Estrada and U. G. Meissner, *Phys. Lett. B* **678**, 90 (2009)
- 36) S. Prelovsek, *et al.* arXiv:1005.0948 [hep-lat]. S. Prelovsek and D. Mohler, *Phys. Rev. D* **79**, 014503 (2009)